Journal of Medicinal Chemistry

pubs.acs.org/jmc

Article

Targeting the Regulatory Site of ER Aminopeptidase 1 Leads to the Discovery of a Natural Product Modulator of Antigen Presentation

John Liddle, Jonathan P. Hutchinson, Semra Kitchen, Paul Rowland, Margarete Neu, Ted Cecconie, Duncan S. Holmes, Emma Jones, Justyna Korczynska, Despoina Koumantou, Jonathan D. Lea, Leng Nickels, Michelle Pemberton, Alex Phillipou, Jessica L. Schneck, Hester Sheehan, Christopher P. Tinworth, Iain Uings, Justyna Wojno-Picon, Robert J. Young, and Efstratios Stratikos*

Cite This: https://dx.doi.org/10.1021/acs.jmedchem.9b02123

Read Online

ACCESS | Metrics & More | Article Recommendations | Supporting Information

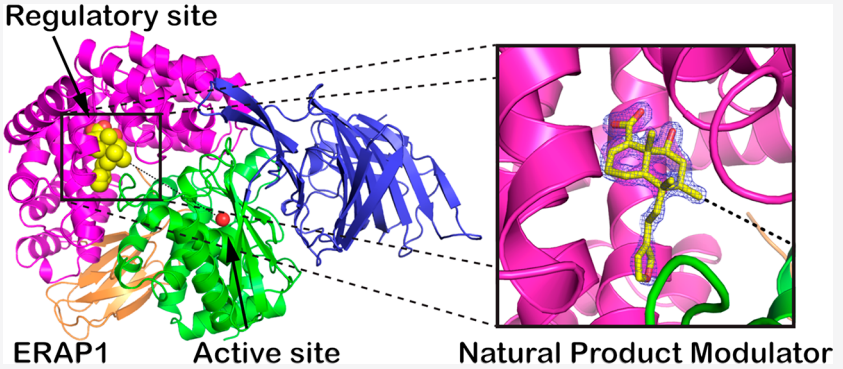

ABSTRACT: ER aminopeptidase 1 (ERAP1) is an intracellular enzyme that generates antigenic peptides and is an emerging target for cancer immunotherapy and the control of autoimmunity. ERAP1 inhibitors described previously target the active site and are limited in selectivity, minimizing their clinical potential. To address this, we targeted the regulatory site of ERAP1 using a high-throughput screen and discovered a small molecule hit that is highly selective for ERAP1. (4a*R*,5*S*,6*R*,8*S*,8a*R*)-5-(2-(Furan-3-yl)ethyl)-8-hydroxy-5,6,8a-trimethyl-3,4,4a,5,6,7,8,8a-octahydronaphthalene-1-carboxylic acid is a natural product found in *Dodonaea viscosa* that constitutes a submicromolar, highly selective, and cell-active modulator of ERAP1. Although the compound activates hydrolysis of small model substrates, it is a competitive inhibitor for physiologically relevant longer peptides. Crystallographic analysis confirmed that the compound targets the regulatory site of the enzyme that normally binds the C-terminus of the peptide substrate. Our findings constitute a novel starting point for the development of selective ERAP1 modulators that have potential for further clinical development.

INTRODUCTION

ER aminopeptidase 1 (ERAP1) is an aminopeptidase that belongs to the oxytocinase subfamily of M1 aminopeptidases.[1] ERAP1 has important functions in the adaptive immune system, with the most prominent one being the preparation of antigenic peptides for presentation by major histocompatibility class I molecules (MHC-I). In this context, ERAP1 trims elongated antigenic peptide precursors that are translocated into the ER by the transporter associated with antigen processing (TAP).[2] While the activity of ERAP1 can help generate important antigenic epitopes, it can also overtrim others, essentially destroying them and thus preventing an effective CD8+ cytotoxic T cell response. By these functions, ERAP1 can influence which antigenic peptides will be presented by MHC-I and can therefore indirectly regulate adaptive immune responses.[3] Although ERAP1 is normally retained inside the ER, it can be secreted under certain conditions and can affect innate immune responses and blood pressure.[4,5]

ERAP1 is polymorphic, and at least 10 distinct haplotypes have been identified in the human population.[6] Large genetic-wide association studies have linked coding SNPs present in these common ERAP1 haplotypes, with predisposition to disease, most notably autoimmunity, usually in epistasis with particular HLA-alleles, strengthening the notion that these effects are mediated by changes in antigen presentation.[7,8] These SNPs induce changes in enzymatic activity and can

Received: December 20, 2019
Published: February 28, 2020

affect antigen presentation in model systems.[9,10] Thus, it appears that genetic variability of the ERAP1 gene leads to enzymes with different enzymatic activities and constitutes an additional component of variability of immune responses that synergizes with the natural variability of MHC-I.[10]

Cancer immune evasion may include misregulation of ERAP1 activity.[8] Tumors often either up-regulate or down-regulate ERAP1, possibly as an evolutionary adaptation during cancer immunoediting processes.[11] A potential mechanism may involve destruction of tumor-associated antigenic peptides by ERAP1.[3,12] In model cancer systems, down-regulation of ERAP1 activity has led to increased antitumor cellular immune responses and has sensitized tumors to immune-checkpoint inhibitor therapy.[3,13,14] Finally, germline eQTL's affecting expression of ERAP1 has been found to be associated with immune cell infiltration to tumors.[15] As a result, ERAP1 is an emerging target for cancer immunotherapy.[16]

Several studies have addressed the development of ERAP1 inhibitors.[17] The most potent reported to date includes phosphinic pseudopeptide transition-state analogues that have been developed to nM affinity and shown to be active in cell-based and *ex vivo* systems.[18−20] Phosphinic pseudopeptides as well as other groups of inhibitors reported all target the enzyme's active site, which is largely conserved between family members, thus limiting the selectivity and potential therapeutic utility of the compounds. Indeed, no potent and highly selective ERAP1 inhibitors targeting the active site have been reported to date, suggesting that alternative discovery approaches may be necessary. In this study, we describe the discovery of an allosteric ERAP1 modulator from a large high-throughput screen designed to target the regulatory site of the enzyme. This compound is a natural product, namely, clerodane acid from *Dodonaea viscosa*. The compound can activate small substrate trimming but inhibit the *in vitro* destruction of a model antigenic epitope by ERAP1, inhibit the *in vitro* generation of an ERAP1-dependent epitope from an elongated precursor, and also block the presentation of this epitope in a cellular assay. Crystallographic and biochemical analyses suggest that it binds in a pocket inside the cavity of ERAP1, 25 Å away from the active site, that constitutes a regulatory site that normally binds the C-terminus of peptide substrates. This compound may constitute a valuable tool for the study of effects of ERAP1 inhibition in the mature immune system and a starting point for the development of clinically useful selective inhibitors.

RESULTS

Discovery of a Compound That Activates ERAP1-Mediated Hydrolysis of Small Peptidic Substrates. We sought to develop small-molecule cellular-active and selective modulators of ERAP1. Previous efforts to develop ERAP1 inhibitors have focused on the Zn-containing active site and have resulted in potent compounds, such as DG013A, but with no or very limited selectivity,[18] a major bottleneck to clinical development.[17] To address this problem, we exploited previous observations that suggested that ERAP1 contains a distinct regulatory site necessary for the processing of large peptides.[21] This site, when occupied by small peptides, has been shown to activate the hydrolysis of small fluorigenic substrates by ERAP1.[9,21,22] We therefore hypothesized that small molecules occupying that site may activate small fluorigenic substrate hydrolysis but inhibit the trimming of endogenous peptidic substrates. Thus, we developed a high-throughput assay to monitor the activation and inhibition of the enzyme. For this assay we used the fluorogenic substrate L-Leu-7-amino-4-trifuoromethylcoumarin (Leu-AFC) which is an analogue of the commonly used L-Leu-7-amino-4-methylcoumarin (Leu-AMC) with superior spectral characteristics which make it more appropriate for a high-throughput screen. Approximately 1.9 million compounds from the GSK collection were screened against recombinant human ERAP1. Compounds that led to activation of Leu-AFC hydrolysis were considered as hits. In this primary data set, GSK849 was flagged as a potential activator of Leu-AFC cleavage at 10 μM, and when subsequently assayed in duplicate at a single concentration of 20 μM, GSK849 showed significant activation (161 and 167%) of ERAP1 mediated Leu-AFC hydrolysis. This compound is a natural product, specifically clerodane acid ((4a*R*,5*S*,6*R*,8-*S*,8a*R*)-5-[2-(furan-3-yl)ethyl]-8-hydroxy-5,6,8a-trimethyl-3,4,4a,6,7,8-hexahydronaphthalene-1-carboxylic acid), found in *Dodonaea viscosa*, a flowering plant that belongs to the soapberry family that has been reported to have medicinal uses.[23,24] The structure of the hit compound (henceforth referred to as compound **1**) was confirmed by NMR and LCMS (see Supporting Information) and is shown in Scheme 1.

Scheme 1. Chemical Structure of Compound 1

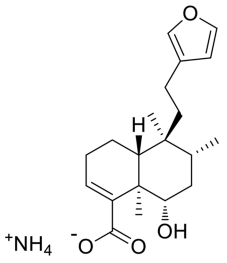

Compound 1 Can Enhance ERAP1 Trimming of Small Substrates by Increasing Substrate Affinity. Compound **1** was able to activate ERAP1 hydrolysis of the frequently used small fluorigenic substrate Leu-AMC[25] by 2- to 2.5-fold and demonstrated submicromolar activity (pIC_{50} = 6.0−6.4 depending on the mathematical model used to fit the data) (Figure 1). It is remarkably selective versus homologous aminopeptidases ERAP2 and IRAP for which it showed weak inhibitory activity at pIC_{50} < 3.8 and pIC_{50} < 3.6, a more than 200- and 600-fold selectivity, respectively (Figure 1A). It has a similar activating effect on the ERAP1-mediated hydrolysis of the small chromogenic substrate leucine-para-nitroanilide (L-pNA) (Figure 1B). Michaelis−Menten analysis data on Leu-pNA hydrolysis (MM analysis using Leu-AMC is complicated by the need to use high concentrations of the substrate that interfere with the signal due to the interfilter effect[21]) were fit to an allosteric-sigmoidal model in accordance to previous studies[21] (Figure 1C). This analysis suggested that compound **1** activates the enzyme by decreasing the K_{prime} value and thus promoting tighter substrate binding (Figure 1D). Given the known effects of conformational changes in ERAP1 activity, we hypothesize that compound **1** may activate hydrolysis of these small substrates by promoting a conformation of the enzyme that can recognize the substrate with higher affinity.[21,26]

Compound 1 Inhibits the Destruction of an Antigenic Epitope by ERAP1. ERAP1 is known to destroy antigenic epitopes by overtrimming them to lengths too short to bind

https://dx.doi.org/10.1021/acs.jmedchem.9b02123
J. Med. Chem. XXXX, XXX, XXX−XXX

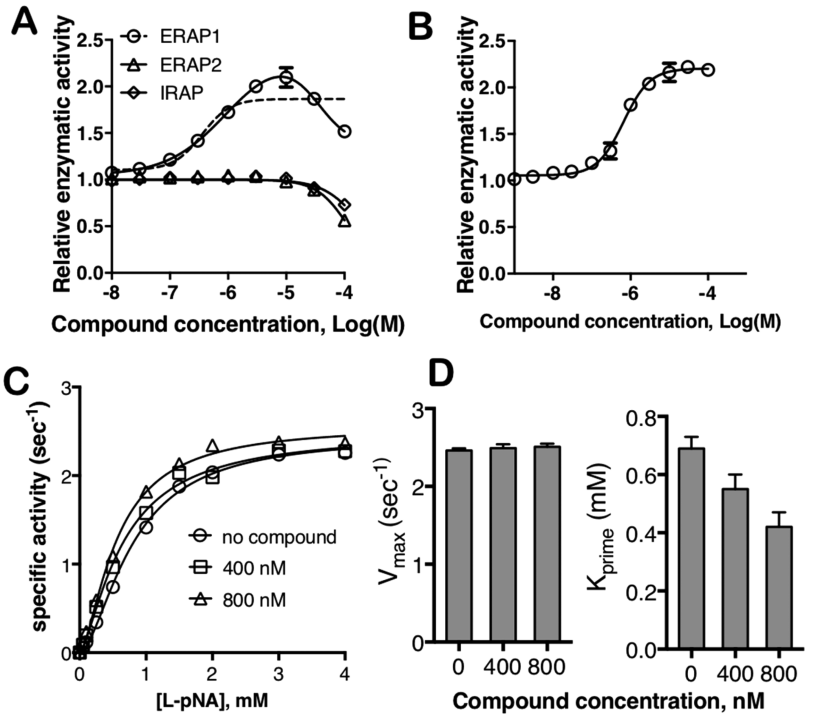

Figure 1. Effects of compound **1** on the hydrolysis of small ERAP1 substrates. (A) Compound **1** activates the hydrolysis of fluorigenic substrate Leu-AMC by ERAP1 but has little effect on hydrolysis of Leu-AMC by the homologous aminopeptidase IRAP or hydrolysis of Arg-AMC by the homologous aminopeptidase ERAP2. Data for ERAP1 were fit to both a dose−response variable slope model (calculated pIC_{50} = 6.4) or a bell-shaped dose−response model (calculated pIC_{50} = 6.0). (B) Compound **1** enhances hydrolysis of chromogenic substrate Leu-pNA (pIC_{50} = 6.2). (C) Michaelis−Menten analysis of Leu-pNA in the presence of 400 or 800 nM compound **1**. Data were fit to an allosteric-sigmoidal model. (D) Effect of compound **1** concentration on V_{max} and K_{prime} parameters calculated from the fits of data in panel C. Compound **1** only affects K_{prime} consistent with an allosteric competitive mechanism of activation. Each data point is the average of three measurements. Error bars indicate standard deviation and are only depicted if larger than the size of the data point, for clarity.

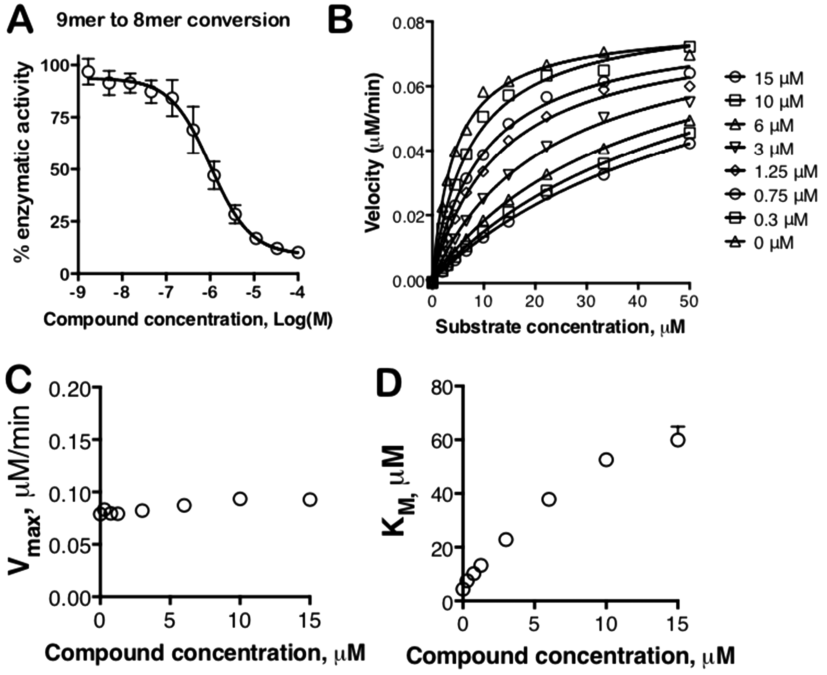

Figure 2. Compound **1** can inhibit the destruction of an antigenic epitope by ERAP1. (A) Dose-dependent inhibition of trimming of 9mer peptide epitope YTAFTIPSI to the 8mer TAFTIPSI. Data were fit to a dose−response variable slope model resulting in a calculated pIC_{50} of 6.0. (B) Michaelis−Menten analysis of inhibition for a range of concentrations of compound **1**, from 0 to 15 μM. (C, D) Calculated V_{max} and K_M values from the model fits shown in panel B. Each data point is the average of three measurements. Error bars indicate standard deviation and are only depicted if larger than the size of the data point, for clarity.

https://dx.doi.org/10.1021/acs.jmedchem.9b02123
J. Med. Chem. XXXX, XXX, XXX−XXX

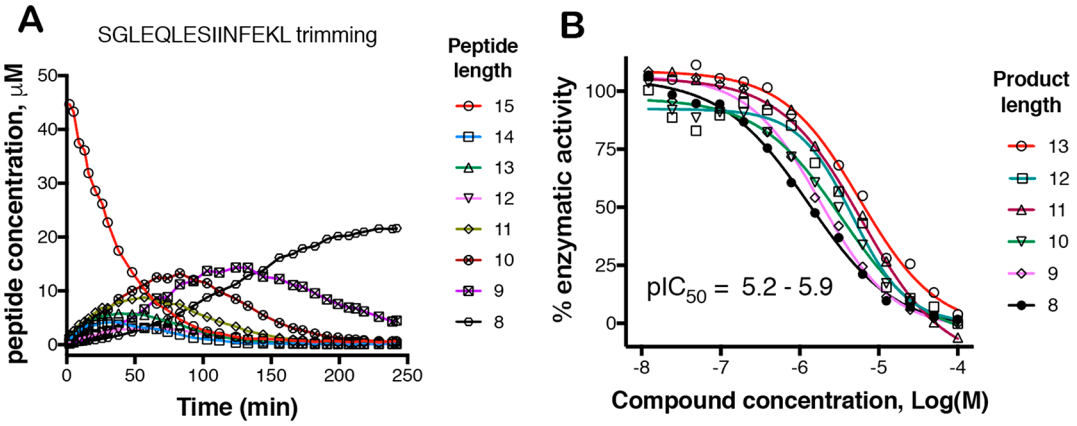

Figure 3. Compound **1** can inhibit processing of a common antigenic peptide precursor from chicken ovalbumin as well as generation of the mature antigenic epitope. (A) Time-course of trimming of a peptide with the sequence SGLEQLESIINFEKL followed by RapidFire MS. All intermediate products are detected, and the mature epitope SIINFEKL accumulates. (B) Dose-dependent inhibition of the generation of products between 8 and 13 amino acids long, by compound **1**.

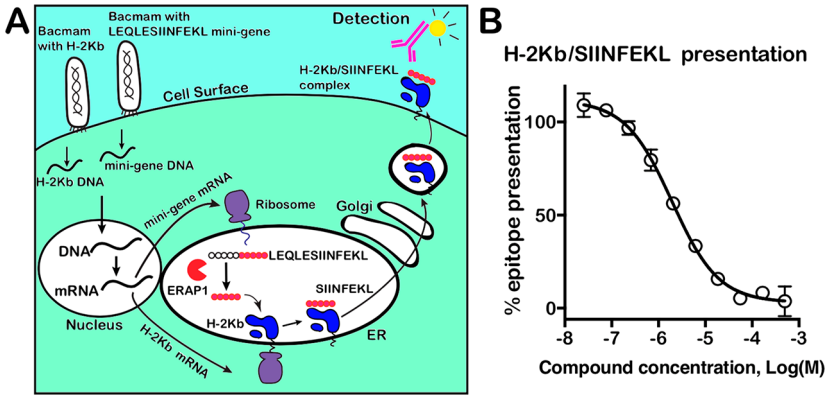

Figure 4. Compound **1** can inhibit the presentation of an ERAP1-dependent epitope by HeLa cells. (A) Schematic representation of cellular assay used. Bacmam vectors carrying DNA coding for the MHC-I allele H-2Kb, beta2m, and a mini-gene that targets the precursor sequence LEQLESIINFEKL to the ER are used to deliver the DNA to HeLa cells. Processing of LEQLESIINFEKL by ERAP1 in the ER is necessary for generation of the mature SIINFEKL sequence that can then be loaded onto nascent H-2Kb. The mature H-2Kb/SIINFEKL complex is then trafficked to the cell-surface, where it can be detected by the conformation-specific antibody 25.D1.16. (B) Titration of compound **1** reduces H-2Kb/SIINFEKL cell-surface presentation with pIC_{50} = 5.7. Each data point is the average of three measurements. Error bars indicate standard error of measurement and are only depicted if larger than the size of the data point, for clarity.

onto MHC-I, and this property has been linked to cancer immune evasion, thus having potential therapeutic applications.[3,12] To characterize the effects of the compound to a more physiologically relevant ERAP1 substrate, we utilized Rapidfire mass spectrometry assay using a 9-amino acid antigenic epitope with the sequence YTAFTIPSI, from Gag-Pol polyprotein from human immunodeficiency virus 1,[27] which we have demonstrated before to be a highly ERAP1-sensitive substrate.[28] The hydrolysis of the tyrosine residue to form TAFTIPSI was monitored by mass spectrometry. In contrast to the single amino acid substrate results, compound **1** showed no evidence of ERAP1 activation with this peptidic substrate up to a concentration of 100 μM but rather showed inhibitory activity with pIC_{50} = 6.0 (Figure 2A). To further investigate this phenomenon, we performed a Michaelis–Menten analysis of the effect of compound **1** on the hydrolysis of the peptide YTAFTIPSI (Figure 2B). The data were fit to the standard Michaelis–Menten (MM) model, which allowed the calculation of the effects of the compound to the enzymatic parameters of the reaction. Overall, the compound acted as a competitive inhibitor, affecting the K_M parameter and not the V_{max} (Figure 2C,D).

Compound 1 Inhibits Processing of an Antigenic Peptide Precursor and Generation of an ERAP1-Dependent Antigenic Epitope. Since one of the main functions of ERAP1 has been reported to be the generation of mature antigenic epitopes from N-terminally elongated precursors,[29] we set up an experimental system to follow the generation of the ovalbumin antigenic epitope with the sequence SIINFEKL using the RapidFire MS system as described in the Experimental Section. We used as an initial substrate a 15mer peptide that includes the SIINFEKL epitope, plus the N-terminal extension SGLEQLE which is the upstream sequence in the ovalbumin protein sequence. Incubation of the 15mer with ERAP1 resulted in the hydrolysis of the starting peptide and subsequent products leading to the accumulation of the 8mer mature epitope (Figure 3A). Interestingly, all possible intermediates were detected at concentrations much greater than the ERAP1 enzyme, which necessitates them being released from the enzyme after each step. This indicates that at least for this reaction, trimming of

https://dx.doi.org/10.1021/acs.jmedchem.9b02123
J. Med. Chem. XXXX, XXX, XXX−XXX

peptides was nonprocessive, consistent with a previous report.[30] We then repeated the reaction in the presence of increasing concentrations of compound **1** and compared the levels of peptides generated (Figure 3B). In all cases the products were reduced in a dose-dependent manner and with pIC_{50} values in the range of 5.2−5.9. Interestingly, inhibition of the generation of SIINFEKL showed the highest pIC_{50}, at 5.9. We conclude that compound **1** can effectively inhibit the generation of an ERAP1-dependent antigenic epitope from an N-terminally extended precursor *in vitro*.

Compound 1 Can Inhibit Antigen Presentation of a Model Epitope. To address the ability of compound **1** to inhibit ERAP1 and affect antigen processing in cells, we utilized a modified version of a previously used antigen presentation assay.[31] This assay reports the cell-surface presentation of the ovalbumin epitope SIINFEKL by the mouse MHC-I allele H-2Kb, a process that is ERAP1-dependent. ER-delivery of a precursor sequence leads to its processing by endogenous ERAP1 and generation of the mature epitope SIINFEKL which is then bound and transported to the cell surface. The assay was designed to deliver both the H-2Kb allele and a mini-gene coding for the ER-targeted precursor sequence LEQLESIINFEKL, after infection of HeLa cells by appropriate BacMam viruses (Figure 4A).[32] In the absence of an inhibitor, infection of HeLa cells by the two BacMam viruses results in high presentation of the H-2Kb/SIINFEKL complex on the cell surface as determined by FACS using the H-2Kb/SIINFEKL specific antibody 25.D1.16. Titrating compound **1** resulted in a dose-dependent reduction of H-2Kb/SIINFEKL complex present on the cell surface with a pIC_{50} = 5.7 (Figure 4B). No effects in cell viability were evident for concentrations up to 167 μM (Supplementary Figure 1). This finding suggests that compound **1** can target ERAP1 in antigen presenting cells and block the generation of an ERAP1-dependent antigenic epitope. Interestingly, the cell-based pIC_{50} value is comparable to the *in vitro* efficacy values, suggesting that compound **1** is very efficient in penetrating the cell and targeting ERAP1 inside the ER. Indeed, the cellular potency of compound **1** is comparable to the potency of the most potent to-date ERAP1 active site inhibitor (DG013A) when measured by a similar assay.[33]

Compound Targets the Regulatory Site of ERAP1. To understand the mechanism of action of compound **1**, especially in the context of its high selectivity versus highly homologous aminopeptidases, we cocrystallized it in complex with ERAP1. Crystals of the complex diffracted to 1.7 Å, and the crystal structure was solved using molecular replacement (Table 1). The enzyme was found to be in the closed conformation with no major changes compared to another recent high-resolution structure described (Figure 5).[34] Residual $F_o - F_c$ density was discovered at a location distant from the active site (Supplementary Figure 2), about 25 Å away, and was used to refine the model using the chemical structure shown in Scheme 1. Refinement was highly consistent with the known structure, confirming that the compound **1** shown in Scheme 1 is indeed the ERAP1 inhibitor. Although the compound acted as a competitive inhibitor versus antigenic peptides and antigenic peptide precursors, its location 25 Å away from the catalytic center (indicated by the presence of the Zn(II) atom) suggests that, at least for small substrates, it should act by an allosteric mechanism.

To confirm that the proposed binding site is indeed the site that confers its activation and inhibitory properties, we

Table 1. Data Collection and Refinement Statistics for Crystal Structure of ERAP1/Compound 1 Complex[a]

data collection resolution range	59.61−1.67 (1.71−1.67)
space group	$P2_12_12$
unit cell [a, b, c (Å); α, β, γ (deg)]	113.22, 140.26, 57.92; 90, 90, 90
total reflections	687070 (51056)
unique reflections	107621 (7863)
multiplicity	6.4 (6.5)
completeness (%)	100.0 (100.0)
mean $I/\sigma(I)$	10.7 (1.5)
Wilson B-factor (Å^2)	26.2
R_{merge}	0.094 (1.042)
$CC_{1/2}$	0.997 (0.474)
refinement resolution range	24.45−1.67 (1.71−1.67)
reflections used in refinement	107497
reflections used for R_{free}	5364
R_{work}	0.169 (0.234)
R_{free}	0.194 (0.226)
number of non-hydrogen atoms	7988
protein	6928
ligands	115
solvent	945
protein residues	856
RMS bonds (Å)	0.010
RMS angles (deg)	0.97
Ramachandran favored (%)	96.9
Ramachandran allowed (%)	99.6
Ramachandran outliers (%)	0.4
rotamer outliers (%)	1.2
clashscore	1.14
average B-factor (Å^2)	31.0
macromolecules	28.7 (main chain 25.6/side chain 31.8)
ligands	41.4
solvent	40.9
number of TLS groups	1

[a]Values for the highest resolution shell are given in parentheses.

generated ERAP1 variants carrying single or double amino acid mutations in residues 684 and 685 which, based on the crystal structure, make key interactions with the carboxylate group of compound **1**. Titrations using these variants and the Leu-AMC substrate showed that the mutations resulted in progressively weaker dose-dependent responses depending on the nature of the mutation (Figure 6A). Specifically, substituting Tyr684 with a phenylalanine reduced the EC_{50} by 1 order of magnitude, whereas substituting Lys685 with an alanine reduced the EC_{50} by more than 2 orders of magnitude, consistent with the nature of interactions between compound **1** and these two residues (one hydrogen bond with Tyr684 versus hydrogen bonds plus electrostatic interactions for Lys685) (Figure 6B). Mutating Lys685 to methionine would produce steric clashes with the inhibitor and resulted in no detectable activity. The double mutant Tyr684Phe/Lys685Ala also abrogated compound **1** activity. These results confirm that the location discovered in the crystal structure is indeed the location conferring compound **1** activity and also that the interactions between residues 684/685 with the carboxylate group in compound **1** are critical for binding and/or activity.

The mechanism that compound **1** utilizes to exert its effects on ERAP1 activity may be understood in the context of existing knowledge of the complex mechanism that ERAP1 utilizes to trim substrates. ERAP1 has been shown to exist in at

https://dx.doi.org/10.1021/acs.jmedchem.9b02123
J. Med. Chem. XXXX, XXX, XXX−XXX

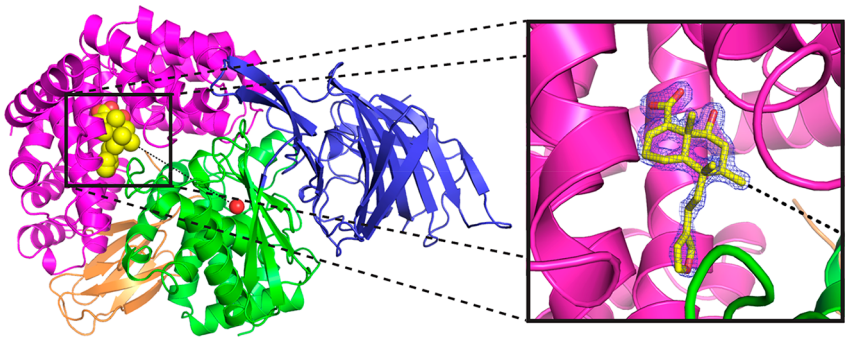

Figure 5. Crystal structure of the complex of compound **1** with ERAP1. On the left part of the figure, ERAP1 is shown in cartoon representation with its four domains colored (domain I in blue, domain II in green, domain III in orange, and domain IV in magenta). The active site zinc(II) atom is indicated by a red sphere. Compound **1** is shown in yellow spheres and in yellow sticks in the zoomed-in representation on the right. Refined $2F_o - F_c$ electron density map is shown as a blue mesh. The closest distance between a methyl group of compound **1** and the zinc(II) atom is shown by a dotted line and represents a distance of 25 Å. The crystal structure has been deposited to the Protein Data Bank (PDB code 6T6R).

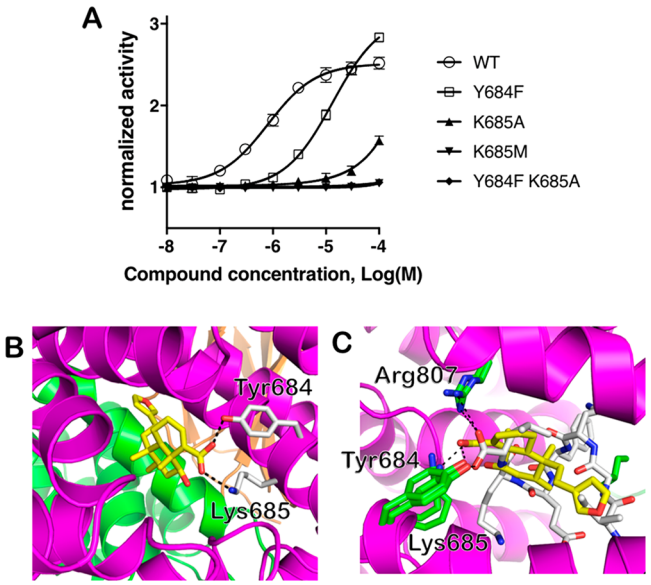

Figure 6. (A) Effect of mutating residues 684 and 685 that make interactions with the carboxyl group of compound **1**, on the ability of the compound to activate the hydrolysis of Leu-AMC by ERAP1. Data points are the average of three measurements, and error bars correspond to standard deviation (shown only if larger than data point, for clarity). (B) Schematic representation of compound **1** (yellow sticks) bound in domain IV of ERAP1 (PDB code 6T6R in magenta cartoon) making interactions through its carboxylate with Tyr684 and Lys685. (C) Compound **1** occupies the same location and makes highly similar interactions with the IINFEKL peptide seen in a crystal structure of the C-terminal domain of ERAP1 (PDB code 5J5E).[37]

least two (and possibly more) conformations, one of them being "closed" in which the active site is excluded from the outside solvent but is part of a large internal cavity.[21,35] An alternative "open" conformation is formed when domain IV moves away from domains I/II using domain III as a hinge. On the basis of the arrangement of catalytic residues and substrate binding pockets, it has been hypothesized that the closed conformation is the active one or at least a more active state.[21] Recent data using small-angle X-ray scattering have suggested that the open conformation may be dominant in solution, and ligand binding may promote the transition from open to closed conformation.[26] Additionally, biochemical analyses have suggested that ERAP1 also contains an allosteric regulatory site, distal from the active site, which, when occupied by peptides, may promote the open-to-closed transition.[36] Indeed, small peptides have been shown to activate Leu-AMC hydrolysis, similar to compound **1**, but to inhibit trimming of larger peptides.[21] Interestingly, the location of this regulatory site has been proposed based on the arrangement of a crystallographic dimer of the C-terminal domain of ERAP1, in which the C-terminal tail of one monomer, which carried the sequence IINFEKL, was found bound in a crevice of the other.[37] Overlay of this structure with the structure of ERAP1 with compound **1** indicates that both the IINFEKL peptide and compound **1** are bound on the same location and their carboxylate groups interact with the same residues, namely, Tyr684, Lys685, and Arg807 (Figure 6C). Indeed, in a recent study, we solved the crystallographic structure of ERAP1 in complex with a 15mer substrate analogue and found its C-terminal moiety anchored at that exact same site.[38] Biochemical and structural analysis confirmed that Tyr684, Lys685, and Arg807 constitute a carboxypeptidase-like structural motif that forms a C-terminus recognition element inside an allosteric pocket that can communicate the binding of the peptide C-terminus to the active site by affecting the molecular dynamics of the enzyme.[38] These observations, taken together, suggest that the activating properties of compound **1** are based on binding in the allosteric-regulatory site of ERAP1, which leads to activation of trimming of small substrates. The situation is however reversed for larger peptidic substrates whose C-terminus also normally occupies the same allosteric regulatory site and thus is out-competed by the compound which, for those substrates, acts as a competitive inhibitor.

DISCUSSION

Although compound **1** was initially discovered as an activator of ERAP1, this appears to be a result of the allosteric site targeted, and this it is not a global activator of the enzyme but rather an inhibitor for physiologically relevant substrates. It has been proposed that ERAP1 preferentially trims large peptides by utilizing a regulatory site that, when concurrently occupied by a sufficiently large peptide, leads to self-activation.[36] Small substrates can occupy the active site at the same time as some small peptides occupy the regulatory site, leading to an apparent activation effect.[21] It appears that compound **1** mimics this effect by selectively binding to the regulatory allosteric site, making the same interactions as the C-terminus

https://dx.doi.org/10.1021/acs.jmedchem.9b02123
J. Med. Chem. XXXX, XXX, XXX−XXX

of the peptide. The situation is reversed however for longer peptides, since compound **1** now competes for the same allosteric site, leading to competitive inhibition. In this context, compound **1** works by utilizing a mechanistic feature of ERAP1 that is unique to this aminopeptidase. Indeed, structural and biochemical analysis of the two most homologous enzymes, ERAP2 and IRAP, has suggested that they do not share ERAP1's selectivity for large peptides, neither a regulatory site that recognizes the C-termini of peptidic substrates.[39,40] Interestingly, although compound **1** targets an allosteric site, it appears to be as efficient in inhibiting ERAP1 in cells as the most potent active-site inhibitor described, suggesting that the regulatory site is equally as druggable in cells as the active site.[33]

The exact mechanism of communication between the regulatory and active sites of ERAP1 is not fully understood. Two main hypotheses have been proposed, both in the context of altering molecular and conformational dynamics of the enzyme. Recent molecular dynamics analysis from our group suggested a direct path of communication between the two sites, based on which, occupancy of the regulatory site stabilizes the dynamics of active site residues.[38] Alternatively, it has been proposed that occupation of the regulatory site can facilitate domain closing and conformational change to the closed, more active conformation.[21,26] It should be noted that these two mechanisms are not mutually exclusive and could operate concurrently or even synergistically. Regardless, if occupation of the regulatory site by a peptide C-terminus leads to closing of the enzyme, it is possible that compound **1** has the exact same effect and thus shifts the equilibrium from the open to the closed state. This would produce an apparent inhibitory effect since the closed conformation cannot allow a new peptide to enter the ERAP1 active site and be cleaved. Either of these two mechanisms, (i) competition for the regulatory site or (ii) stabilizing the closed conformation, could underlie the inhibitory properties of compound **1**. The discovery of compound **1** could thus be a very useful tool for future studies aiming to understand the exact mechanism that regulates ERAP1 activity and substrate selection.

The ability of compound **1** to inhibit trimming of N-terminally elongated SIINFEKL precursors both *in vitro* and in cells also provides insight on the mechanism of function of ERAP1 in cells. The engagement of the regulatory site by the C-terminus of the peptide substrate has been shown to be important for trimming of long peptides in solution.[21,30,38] However, ERAP1 has been proposed to be able to also trim peptides while they are still bound onto the MHCI by their C-terminus, a controversial mechanism that is inconsistent with binding of the peptide C-terminus by ERAP1.[41−43] If ERAP1 were to trim antigenic peptide precursors while their C-terminus is still bound on MHCI, compound **1** should be inefficient as an inhibitor. Thus, the ability of compound **1** to inhibit ERAP1-trimming in cells suggests that, at least for this group of antigenic peptide precursors, engagement of the peptide C-terminus by ERAP1 is necessary in cells and on-MHCI trimming is either not utilized or not required.

Despite significant efforts reported in the development of ERAP1 inhibitors during the past few years, targeting the enzyme active site has failed to produce compounds of sufficient potency and selectivity versus other homologous members of the M1 aminopeptidase family.[17] In a recent study published during the preparation of this manuscript, ERAP1 inhibitors with selectivity versus ERAP2 and IRAP were disclosed but were not as potent as previously developed compounds.[44] Given the complex and varied biological functions of this aminopeptidase family, lack of selectivity may pose a major hurdle to any clinical development. This observation is highlighted for the case of IRAP, which is targeted by virtually all previously reported ERAP1 inhibitors, while having a multitude of biological functions.[45] To circumvent these problems, we describe here a *de novo* high-throughput approach that focuses on the regulatory site of ERAP1. We report a submicromolar natural product allosteric modulator of ERAP1 that is selective versus its two most homologous enzymes, ERAP2 and IRAP. Allosteric modulators represent a promising alternative approach to inhibitor design and offer opportunities for enhanced selectivity since they do not target conserved structural features between enzymes. Furthermore, the compound described here is low MW and shows cellular activity that matches in potency the *in vitro* activity, suggesting that it can easily penetrate cells. As a result, it represents a promising hit compound for further development as a tool to regulate antigen presentation for therapeutic applications and could itself constitute a useful tool compound for interrogating molecular aspects of intracellular antigen processing. Indeed, the effects of ERAP1 inhibition on the immunopeptidome (the sum of peptides presented by MHC-I) of cancer cells have been recently investigated using the inhibitor DG013A, which, albeit potent, is not selective.[18] Although significant changes in the immunopeptidome were detected that could be exploitable for cancer immunotherapy applications, possible off-target effects complicated interpretation.[33] Future experiments will have to address these concerns using the more selective compound **1**, as well as possible effects on the immunopeptidome by targeting the C-terminus binding site of ERAP1 versus targeting the N-terminus binding/active site.

CONCLUSION

We describe the discovery and characterization of a natural product modulator of ERAP1 that can activate the hydrolysis of small model substrates while inhibiting both the destruction and generation of antigenic epitopes. This compound constitutes a novel strategy for inhibiting ERAP1 by targeting the recognition of the C-terminus of the substrate, in contrast to other previously reported ERAP1 inhibitors that target the active site. The novel mechanism and selectivity of this compound represent a unique opportunity for the development of clinically useful ERAP1 inhibitors that aim to regulate the cellular immunopeptidome for applications in cancer immunotherapy or control of autoimmunity.

EXPERIMENTAL SECTION

Materials. 25.D1.16 antibody conjugated to APC (SIINFEKL-H-2kb APC antibody) was purchased from Thermo Fisher (catalog no. 17-5743-82). Mouse H-2kb/beta2m BacMam, LEQLESIINFEKL GFP BacMam and KKSIINFEKL GFP BacMam were purchased from Genscript. HeLa cells were from Biocat (catalog no. 1148), DMEM/F12 was from Sigma (catalog no. D6421), and heat inactivated FBS was from Gibco (catalog no. 10099-141). Peptides were synthesized by Biopeptide Inc. and Cambridge Research Biochemicals Ltd., purified by HPLC to greater than 95% purity, and validated by MS. Leu-AMC, Arg-AMC, and Leu-pNA were purchased from Sigma-Aldrich. Leu-AFC was purchased from Cambridge Research Biochemicals.

Compound Sourcing and Characterization. Compound **1** was purchased from AnalytiCon Discovery GmbH (catalog no. NP-

https://dx.doi.org/10.1021/acs.jmedchem.9b02123
J. Med. Chem. XXXX, XXX, XXX−XXX

008402). Purification was conducted on an XBridge Phenyl column (30 mm × 150 mm, 5 μm packing diameter) at ambient temperature. The solvents employed were the following: A = 10 mM ammonium bicarbonate in water adjusted to pH 10 with ammonia solution; B = acetonitrile. The gradient employed was as follows:

time (min)	flow rate (mL/min)	% A	% B
0	40	85	15
4.5	40	85	15
20	40	65	35
21	40	60	40
25	40	0	100

The UV detection was an averaged signal from wavelength of 210−350 nm, and mass spectra were recorded on a Waters QDa mass spectrometer using positive electrospray ionization (ES +ve). The appropriate fractions were combined and concentrated under a stream of nitrogen to give the ammonium salt of compound **1** as a white solid. NMR spectra and LCMS traces can be found in Supplementary Figures 3−13.

(4a*R*,5*S*,6*R*,8*S*,8a*R*)-5-(2-(Furan-3-yl)ethyl)-8-hydroxy-5,6,8a-trimethyl-3,4,4a,5,6,7,8,8a-octahydronaphthalene-1-carboxylic Acid. ^{1}H NMR (600 MHz, DMSO-d_6) δ 7.52 (t, J = 1.7 Hz, 1H), 7.42 (s, 1H), 6.48−6.45 (m, 1H), 6.36−6.34 (m, 1H), 3.35 (dd, J = 4.8, 11.0 Hz, 1H), 2.27−2.20 (m, 1H), 2.15−1.99 (m, 3H), 1.66−1.53 (m, 3H), 1.52−1.30 (m, 4H), 1.22 (d, J = 11.7 Hz, 1H), 1.11 (s, 3H), 0.77 (d, J = 6.6 Hz, 3H), 0.66 (s, 3H). Alcohol OH not observed, ammonium peak not resolved. ^{13}C NMR (151 MHz, DMSO-d_6) δ 173.30, 148.46, 142.87, 138.52, 132.06, 125.29, 111.17, 73.88, 45.22, 44.39, 38.57, 38.21, 36.57, 33.30, 26.48, 17.53, 17.41, 17.36, 16.88, 15.73. Reported to two decimal places to differentiate the signals. NMR purity >95%. LCMS (ES −ve) m/z 331.3 $(M - H)^-$ t_R = 0.85 min (91% a/a, potentially modest chromophore. NMR indicates >95% purity).

Nuclear Magnetic Resonance (NMR). NMR spectra were recorded using a Bruker AVIII600 (with cryoprobe). Chemical shifts (δ) are reported in parts per million (ppm) relative to tetramethylsilane, and coupling constants (J) are in Hz. The following abbreviations are used for multiplicities: s = singlet; br. s = broad singlet; d = doublet; t = triplet; q = quartet; spt = septet; m = multiplet; dd = doublet of doublets. If not specifically stated, the NMR experiments were run at 30 °C.

Liquid Chromatography−Mass Spectroscopy (LCMS). The analysis was conducted on an XBridge C18 column (50 mm × 4.6 mm internal diameter 3.5 μm packing diameter) at 30 °C. The solvents employed were the following: A = 10 mM ammonium bicarbonate in water adjusted to pH 10 with ammonia solution; B = acetonitrile. The typical gradient employed was as follows:

time (min)	flow rate (mL/min)	% A	% B
0	1	97	3
0.05	1	97	3
1.50	1	5	95
1.90	1	5	95
2.00	1	97	3

The UV detection was an averaged signal from wavelength of 210−350 nm, and mass spectra were recorded on a Waters ZQ mass spectrometer using alternate-scan positive and negative mode electrospray ionization (ES +ve and ES −ve).

***In Vitro* Enzymatic Assays.** The enzymatic assays using Leu-AMC and Leu-pNA (both from Sigma-Aldrich) have been described before.[26] The HTS assay was run at 4 μL/well in 1536-well format, using Leu-AFC as substrate (an analogue of Leu-AMC with superior spectral characteristics). The HTS assay was run in a buffer of 50 mM Hepes (pH 7.0), 100 mM NaCl, 0.002% Tween-20, 0.005% BSA, using a final concentration of 5 nM ERAP1 and 50 μM Leu-AFC. After a 60 min reaction time, plates were quenched by the addition of TFA to a final concentration of 0.25%. Fluorescence intensity was measured using a PerkinElmer Envision plate reader. The Rapidfire MS assays were run in the same buffer at 25 μL/well in 384-well format, using a Rapidfire autosampler (Agilent) equipped with a C18 solid phase cartridge, coupled to a Sciex 4000 Q-trap MS (AB Sciex). For the assay using YTAFTIPSI as substrate, final concentrations of 1 nM ERAP1 and 5 μM substrate were incubated with test compound for 60 min. Control wells comprised high control (no inhibitor = 0% inhibition) and low control (no enzyme = 100% inhibition). Reactions were quenched by addition of TFA including internal standard peptide Ac-YTAFTIPSI, to give final concentrations of 0.375% and 2.5 μM, respectively. Integrated signals for product (TAFTIPSI) and internal standard (Ac-YTAFTIPSI) were measured, and the product data were normalized by dividing by the internal standard data. Normalized data were then converted either to % inhibition using 100(high − sample)/(high − low) or to % activity using 100(sample − low)/(high − low). Data were then fitted to a four-parameter dose−response model to determine pIC_{50}, Hill slope, minimum asymptote, and maximum asymptote. The Michaelis−Menten analysis was performed similarly, using an ERAP1 concentration of 1 nM. Reactions were quenched at time points of 15, 30, 45, and 60 min. Data were normalized to internal standard as above and then converted to [product] using a standard curve of TAFTIPSI. Initial rates were obtained from the gradients of the kinetic data. The time course of SGLEQLESIINFEKL trimming was run at 10 nM ERAP1/25 μM peptide as a 50 μL/well assay and quenched by addition of TFA to a final concentration of 0.375%. Concentrations of each peptide species were determined by reference to standard curves for each peptide. The corresponding inhibition experiment was run at 10 nM ERAP1/25 μM GLEQLESIINFEKL as a 25 μL/well assay and quenched after 30 min. Concentrations of each peptide species were obtained from standard curves and converted to % activity and fitted as described above.

Cell-Based Assay. The cell-based assay used to evaluate the effect of the compound on antigen presentation in cells is based on specific recognition of the ovalbumin epitope SIINFEKL when presented by the mouse MHCI H-2Kb by the antibody 25.D1.16 conjugated with allophycocyanin (APC). The assay was run in a 96-well plate format, using Cellstar 96U TC plates (Greiner), and read on a Beckman Coulter Cyan flow cytometer. Two BacMam vectors, one encoding a precursor version of SIINFEKL (sequence LEQLESIINFEKL) and another encoding mouse MHC-I (H-2Kb and beta2m), were incubated with HeLa cells and compound for 40 h. Peptides encoded by the BacMams were translocated into the ER by means of signal peptide sequences. The LEQLESIINFEKL precursor was processed by endogenous ERAP1, resulting in the removal of the two N-terminal leucine residues and generation of SIINFEKL, which then bound onto H-2Kb/beta2m complexes and were translocated to the cell surface for detection by the APC-conjugated antibody. APC fluorescence was recorded at 665 nm after excitation at 533 nm. A peptide precursor with the sequence KKSIINFEKL was also included in a separate BacMam as a control. Since lysine residues are poor substrates for ERAP1, this substrate led to no SIINFEKL production or signal detection The LEQLESIINFEKL and KKSIINFEKL BacMam vectors also encoded GFP on a separate cassette, which was used as a marker of successful BacMam transduction and protein expression. Cell viability was evaluated using the Zombie Violet dye using excitation at 405 nm and emission at 450 nm. A threshold of 95% cell viability was used to determine DMSO tolerance, which was set to 0.5% DMSO. For normalization of the data the following equation was used: signal = 100 × (compound − control 2)/(control 1 − control 2), where control 1 is cells transduced with LEQLESIINFEKL + DMSO and control 2 is cells transduced with KKSIINFEKL + DMSO. Normalized data were fit to a four-parameter variable slope dose-dependence model, used to calculate PIC_{50} values.

Protein Construct. For screening and assays, full-length ERAP1 was used with a sequence corresponding to the common haplotype 2 with an additional C-terminal 6His-tag.[6] ERAP1 variants (Lys685Met, Lys685Ala, Tyr684Phe, Tyr684Phe-Lys685Ala) were generated by site directed mutagenesis using the haplotype 2 construct as a DNA template. The following primers were used to introduce the mutations: 5′-TTCCTATGTATGCGTTAATGGAGAAA-

https://dx.doi.org/10.1021/acs.jmedchem.9b02123
J. Med. Chem. XXXX, XXX, XXX−XXX

AGAGATAT and 3′-TCTCCATTAACGCATACATAGGAATCAGCTCATT for Lys685Met variant, 5′-TCCTATGTATATGTTAATGGAGAAAAGAGATAT and 3′-TCTCCATTAACATATACATAGGAATCAGCTCAT for Lys685Ala variant, 5′-ATGAGCTGATTCCTATGTTTAAGTTAATGGAGAAAAGAGATATGAATG and 3′-TCTTTTCTCCATTAACTTAAACATAGGAATCAGCTCATTCAAACCTTGAA for Tyr684Phe variant, and 5′-GAGCTGATTCCTATGTTTGCGTTAATGGAGAAAAGAGATATGAATG and 3′-ATCTCTTTTCTCCATTAACGCAAACATAGGAATCAGCTCATTCAAACCTTGAAAC for Tyr684Phe/Lys685Ala variant. For X-ray structure determination, we further optimized our initial crystallization construct as described before[34] by removing amino acids 486−513 which form a disordered loop and by replacing Asn residues 70, 154, 414, 760 with Gln to remove the glycosylation sites. For all constructs protein expression was performed as previously described, with the exception that the C-terminal His tag was not removed for screening and mechanism studies.[34]

Crystallization and Data Collection. Crystals of human ERAP1 were grown at 20 °C by vapor diffusion using a protein concentration of 9.4 mg/mL in protein buffer 50 mM Hepes, pH 7.0, 150 mM NaCl. The protein was prepared by adding 0.2 μL of a 100 mM compound stock solution in DMSO to 30 μL of protein to give a resulting solution of approximately 0.7 mM compound and 0.7% DMSO concentration (~7.5× excess over the protein concentration). For cocrystallization a standard PACT screen (Molecular Dimensions) was used in a 96-well MRC 2-well sitting drop crystallization plate with 80 μL of reservoir solutions. Crystallization drops were set up using a Mosquito robot with two different protein to crystallization solution drop ratios (100 nL of protein + 100 nL of crystallization solution and 100 nL of protein + 50 nL of crystallization solution). The crystal used for X-ray data collection was harvested from PACT condition D1 (0.1 M MMT, pH 4.0, 25% PEG 1500), MMT = DL-malic acid, MES monohydrate, Tris. Crystals were frozen in liquid nitrogen using a cryoprotectant of 20% ethylene glycol mixed with the reservoir solution. X-ray diffraction data were collected at 100 K at the European Synchrotron Radiation Facility (ESRF). The data were processed and scaled with the ESRF automated beamline data processing software, using DIALS,[46] AIMLESS,[47] and the CCP4 suite of programs.[48]

Structure Determination and Refinement. The structure was determined using the coordinates of an isomorphous unliganded protein model (unpublished), with preliminary refinement carried out using autoBUSTER.[49] The ligand was clearly visible in the resulting $F_o - F_c$ electron density map (Supplementary Figure 1). Model building was carried out with Coot[50] using a ligand dictionary generated from grade (Global Phasing Ltd.). Final refinement was carried out using autoBUSTER. Data collection statistics and refinement details for the final model are given in Table 1. The coordinates and structure factors have been deposited in the Protein Data Bank under the accession code 6T6R.

■ ASSOCIATED CONTENT

Supporting Information

The Supporting Information is available free of charge at https://pubs.acs.org/doi/10.1021/acs.jmedchem.9b02123.

Cell viability titration; electron density difference map in the inhibitor binding site; ^{1}H NMR, ^{13}C NMR, HSQC, HMBC, and COSY spectra of compound **1**; NMR correlation summary; LCMS trace (PDF)

Molecular formula strings and some data (CSV)

Accession Codes

Atomic coordinates and structure factors have been deposited in the Protein Data Bank as entry 6T6R. Authors will release the atomic coordinates upon article publication.

■ AUTHOR INFORMATION

Corresponding Author

Efstratios Stratikos − *National Centre for Scientific Research "Demokritos", Athens 15341, Greece;* orcid.org/0000-0002-3566-2309; Phone: (+30) 2106503918; Email: stratos@rrp.demokritos.gr; Fax: (+30)2106503918

Authors

John Liddle − *Discovery Partnerships with Academia, GlaxoSmithKline, Stevenage, Hertfordshire SG1 2NY, U.K.*

Jonathan P. Hutchinson − *Medicinal Science and Technology, GlaxoSmithKline, Stevenage, Hertfordshire SG1 2NY, U.K.*

Semra Kitchen − *Discovery Partnerships with Academia, GlaxoSmithKline, Stevenage, Hertfordshire SG1 2NY, U.K.*

Paul Rowland − *Medicinal Science and Technology, GlaxoSmithKline, Stevenage, Hertfordshire SG1 2NY, U.K.*

Margarete Neu − *Medicinal Science and Technology, GlaxoSmithKline, Stevenage, Hertfordshire SG1 2NY, U.K.*

Ted Cecconie − *Medicinal Science and Technology, GlaxoSmithKline, Collegeville, Pennsylvania 19426, United States*

Duncan S. Holmes − *Discovery Partnerships with Academia, GlaxoSmithKline, Stevenage, Hertfordshire SG1 2NY, U.K.*

Emma Jones − *Medicinal Science and Technology, GlaxoSmithKline, Stevenage, Hertfordshire SG1 2NY, U.K.*

Justyna Korczynska − *Medicinal Science and Technology, GlaxoSmithKline, Stevenage, Hertfordshire SG1 2NY, U.K.*

Despoina Koumantou − *National Centre for Scientific Research "Demokritos", Athens 15341, Greece;* orcid.org/0000-0002-9203-9900

Jonathan D. Lea − *Medicinal Science and Technology, GlaxoSmithKline, Stevenage, Hertfordshire SG1 2NY, U.K.*

Leng Nickels − *Medicinal Science and Technology, GlaxoSmithKline, Collegeville, Pennsylvania 19426, United States*

Michelle Pemberton − *Medicinal Science and Technology, GlaxoSmithKline, Stevenage, Hertfordshire SG1 2NY, U.K.*

Alex Phillipou − *Medicinal Science and Technology, GlaxoSmithKline, Stevenage, Hertfordshire SG1 2NY, U.K.*

Jessica L. Schneck − *Medicinal Science and Technology, GlaxoSmithKline, Collegeville, Pennsylvania 19426, United States*

Hester Sheehan − *Medicinal Science and Technology, GlaxoSmithKline, Stevenage, Hertfordshire SG1 2NY, U.K.*

Christopher P. Tinworth − *Medicinal Science and Technology, GlaxoSmithKline, Stevenage, Hertfordshire SG1 2NY, U.K.;* orcid.org/0000-0002-2756-707X

Iain Uings − *Discovery Partnerships with Academia, GlaxoSmithKline, Stevenage, Hertfordshire SG1 2NY, U.K.*

Justyna Wojno-Picon − *Medicinal Science and Technology, GlaxoSmithKline, Stevenage, Hertfordshire SG1 2NY, U.K.*

Robert J. Young − *Medicinal Science and Technology, GlaxoSmithKline, Stevenage, Hertfordshire SG1 2NY, U.K.;* orcid.org/0000-0002-7763-0575

Complete contact information is available at: https://pubs.acs.org/10.1021/acs.jmedchem.9b02123

Author Contributions

T.C., M.P., J.S., and H.S. performed screening with the Rapidfire MS assay and hit confirmation. J.S.H. and D.K. performed in vitro enzymatic analysis for mechanism of action studies. E.J. and J.K. generated the constructs and protein for screening and assays. S.K. and J.D.L. developed the cell-based

https://dx.doi.org/10.1021/acs.jmedchem.9b02123
J. Med. Chem. XXXX, XXX, XXX−XXX

antigen presentation assay. M.N. and P.R. performed crystallization, solved the crystal structure, and interpreted results. L.N. developed the fluorigenic HTS assay and performed screening. J.D.L. and A.P. performed cell-based assays. C.P.T. purified and characterized the compound. I.U. and J.S. developed strategy for HTS and hit triaging. R.J.Y. and J.W.P. characterized initial hit data and performed subsequent profiling. J.L., I.U., D.H., and E.S. developed research strategy and interpreted results. E.S. wrote the manuscript with help from all authors.

Notes

The authors declare no competing financial interest.

■ ABBREVIATIONS USED

ERAP1, endoplasmic reticulum aminopeptidase 1; ERAP2, endoplasmic reticulum aminopeptidase 2; IRAP, insulin-regulated aminopeptidase; MHC-I, major histocompatibility class I; TAP, transporter associated with antigen processing; Leu-AFC, L-Leu-7-amino-4-trifuoromethylcoumarin; Leu-AMC, L-leucine-7-amido-4-methylcoumarin; Leu-pNA, L-leucine-para-nitroanilide; MM, Michaelis−Menten; Arg-AMC, L-arginine-7-amido-4-methylcoumarin; LCMS, liquid chromatography−mass spectroscopy; MS, mass spectroscopy; APC, allophycocyanin

■ REFERENCES

(1) Tsujimoto, M.; Hattori, A. The oxytocinase subfamily of m1 aminopeptidases. *Biochim. Biophys. Acta, Proteins Proteomics* **2005**, *1751*, 9−18.

(2) Weimershaus, M.; Evnouchidou, I.; Saveanu, L.; van Endert, P. Peptidases trimming mhc class i ligands. *Curr. Opin. Immunol.* **2013**, *25*, 90−96.

(3) James, E.; Bailey, I.; Sugiyarto, G.; Elliott, T. Induction of protective antitumor immunity through attenuation of eraap function. *J. Immunol.* **2013**, *190*, 5839−5846.

(4) Hisatsune, C.; Ebisui, E.; Usui, M.; Ogawa, N.; Suzuki, A.; Mataga, N.; Takahashi-Iwanaga, H.; Mikoshiba, K. Erp44 exerts redox-dependent control of blood pressure at the er. *Mol. Cell* **2015**, *58*, 1015−1027.

(5) Fruci, D.; Romania, P.; D'Alicandro, V.; Locatelli, F. Endoplasmic reticulum aminopeptidase 1 function and its pathogenic role in regulating innate and adaptive immunity in cancer and major histocompatibility complex class i-associated autoimmune diseases. *Tissue Antigens* **2014**, *84*, 177−186.

(6) Ombrello, M. J.; Kastner, D. L.; Remmers, E. F. Endoplasmic reticulum-associated amino-peptidase 1 and rheumatic disease: Genetics. *Curr. Opin. Rheumatol.* **2015**, *27*, 349−356.

(7) Lopez de Castro, J. A.; Alvarez-Navarro, C.; Brito, A.; Guasp, P.; Martin-Esteban, A.; Sanz-Bravo, A. Molecular and pathogenic effects of endoplasmic reticulum aminopeptidases erap1 and erap2 in mhc-i-associated inflammatory disorders: Towards a unifying view. *Mol. Immunol.* **2016**, *77*, 193−204.

(8) Stratikos, E.; Stamogiannos, A.; Zervoudi, E.; Fruci, D. A role for naturally occurring alleles of endoplasmic reticulum aminopeptidases in tumor immunity and cancer pre-disposition. *Front. Oncol.* **2014**, *4*, 363.

(9) Evnouchidou, I.; Kamal, R. P.; Seregin, S. S.; Goto, Y.; Tsujimoto, M.; Hattori, A.; Voulgari, P. V.; Drosos, A. A.; Amalfitano, A.; York, I. A.; Stratikos, E. Coding single nucleotide polymorphisms of endoplasmic reticulum aminopeptidase 1 can affect antigenic peptide generation in vitro by influencing basic enzymatic properties of the enzyme. *J. Immunol.* **2011**, *186*, 1909−1913.

(10) Reeves, E.; Edwards, C. J.; Elliott, T.; James, E. Naturally occurring erap1 haplotypes encode functionally distinct alleles with fine substrate specificity. *J. Immunol.* **2013**, *191*, 35−43.

(11) Fruci, D.; Giacomini, P.; Nicotra, M. R.; Forloni, M.; Fraioli, R.; Saveanu, L.; van Endert, P.; Natali, P. G. Altered expression of endoplasmic reticulum aminopeptidases erap1 and erap2 in transformed non-lymphoid human tissues. *J. Cell. Physiol.* **2008**, *216*, 742−749.

(12) Keller, M.; Ebstein, F.; Burger, E.; Textoris-Taube, K.; Gorny, X.; Urban, S.; Zhao, F.; Dannenberg, T.; Sucker, A.; Keller, C.; Saveanu, L.; Kruger, E.; Rothkotter, H. J.; Dahlmann, B.; Henklein, P.; Voigt, A.; Kuckelkorn, U.; Paschen, A.; Kloetzel, P. M.; Seifert, U. The proteasome immunosubunits, pa28 and er-aminopeptidase 1 protect melanoma cells from efficient mart-126-35-specific t-cell recognition. *Eur. J. Immunol.* **2015**, *45*, 3257−3268.

(13) Cifaldi, L.; Lo Monaco, E.; Forloni, M.; Giorda, E.; Lorenzi, S.; Petrini, S.; Tremante, E.; Pende, D.; Locatelli, F.; Giacomini, P.; Fruci, D. Natural killer cells efficiently reject lymphoma silenced for the endoplasmic reticulum aminopeptidase associated with antigen processing. *Cancer Res.* **2011**, *71*, 1597−1606.

(14) Manguso, R. T.; Pope, H. W.; Zimmer, M. D.; Brown, F. D.; Yates, K. B.; Miller, B. C.; Collins, N. B.; Bi, K.; LaFleur, M. W.; Juneja, V. R.; Weiss, S. A.; Lo, J.; Fisher, D. E.; Miao, D.; Van Allen, E.; Root, D. E.; Sharpe, A. H.; Doench, J. G.; Haining, W. N. In vivo crispr screening identifies ptpn2 as a cancer immunotherapy target. *Nature* **2017**, *547*, 413−418.

(15) Lim, Y. W.; Chen-Harris, H.; Mayba, O.; Lianoglou, S.; Wuster, A.; Bhangale, T.; Khan, Z.; Mariathasan, S.; Daemen, A.; Reeder, J.; Haverty, P. M.; Forrest, W. F.; Brauer, M.; Mellman, I.; Albert, M. L. Germline genetic polymorphisms influence tumor gene expression and immune cell infiltration. *Proc. Natl. Acad. Sci. U. S. A.* **2018**, *115*, E11701−E11710.

(16) Stratikos, E. Modulating antigen processing for cancer immunotherapy. *Oncoimmunology* **2014**, *3*, No. e27568.

(17) Georgiadis, D.; Mpakali, A.; Koumantou, D.; Stratikos, E. Inhibitors of er aminopeptidase 1 and 2: From design to clinical application. *Curr. Med. Chem.* **2019**, *26*, 2715−2729.

(18) Zervoudi, E.; Saridakis, E.; Birtley, J. R.; Seregin, S. S.; Reeves, E.; Kokkala, P.; Aldhamen, Y. A.; Amalfitano, A.; Mavridis, I. M.; James, E.; Georgiadis, D.; Stratikos, E. Rationally designed inhibitor targeting antigen-trimming aminopeptidases enhances antigen presentation and cytotoxic t-cell responses. *Proc. Natl. Acad. Sci. U. S. A.* **2013**, *110*, 19890−19895.

(19) Kokkala, P.; Mpakali, A.; Mauvais, F. X.; Papakyriakou, A.; Daskalaki, I.; Petropoulou, I.; Kavvalou, S.; Papathanasopoulou, M.; Agrotis, S.; Fonsou, T. M.; van Endert, P.; Stratikos, E.; Georgiadis, D. Optimization and structure-activity relationships of phosphinic pseudotripeptide inhibitors of aminopeptidases that generate antigenic peptides. *J. Med. Chem.* **2016**, *59*, 9107−9123.

(20) Chen, L.; Ridley, A.; Hammitzsch, A.; Al-Mossawi, M. H.; Bunting, H.; Georgiadis, D.; Chan, A.; Kollnberger, S.; Bowness, P. Silencing or inhibition of endoplasmic reticulum aminopeptidase 1 (erap1) suppresses free heavy chain expression and th17 responses in ankylosing spondylitis. *Ann. Rheum. Dis.* **2016**, *75*, 916−923.

(21) Nguyen, T. T.; Chang, S. C.; Evnouchidou, I.; York, I. A.; Zikos, C.; Rock, K. L.; Goldberg, A. L.; Stratikos, E.; Stern, L. J. Structural basis for antigenic peptide precursor processing by the endoplasmic reticulum aminopeptidase erap1. *Nat. Struct. Mol. Biol.* **2011**, *18*, 604−613.

(22) Gandhi, A.; Lakshminarasimhan, D.; Sun, Y.; Guo, H. C. Structural insights into the molecular ruler mechanism of the endoplasmic reticulum aminopeptidase erap1. *Sci. Rep.* **2011**, *1*, 186.

(23) Felger, R. S.; Moser, M. B. *People of the Desert and Sea Ethnobotany of the Seri Indians*; The University of Arizona Press: Tucson, AZ, U.S., 2016.

(24) Niu, H. M.; Zeng, D. Q.; Long, C. L.; Peng, Y. H.; Wang, Y. H.; Luo, J. F.; Wang, H. S.; Shi, Y. N.; Tang, G. H.; Zhao, F. W. Clerodane diterpenoids and prenylated flavonoids from dodonaea viscosa. *J. Asian Nat. Prod. Res.* **2010**, *12*, 7−14.

(25) Zervoudi, E.; Papakyriakou, A.; Georgiadou, D.; Evnouchidou, I.; Gajda, A.; Poreba, M.; Salvesen, G. S.; Drag, M.; Hattori, A.; Swevers, L.; Vourloumis, D.; Stratikos, E. Probing the s1 specificity

https://dx.doi.org/10.1021/acs.jmedchem.9b02123
J. Med. Chem. XXXX, XXX, XXX−XXX

pocket of the aminopeptidases that generate antigenic peptides. *Biochem. J.* **2011**, *435*, 411−420.
(26) Stamogiannos, A.; Maben, Z.; Papakyriakou, A.; Mpakali, A.; Kokkala, P.; Georgiadis, D.; Stern, L. J.; Stratikos, E. Critical role of interdomain interactions in the conformational change and catalytic mechanism of endoplasmic reticulum aminopeptidase 1. *Biochemistry* **2017**, *56*, 1546−1558.
(27) Shankar, P.; Russo, M.; Harnisch, B.; Patterson, M.; Skolnik, P.; Lieberman, J. Impaired function of circulating HIV-specific cd8(+) t cells in chronic human immunodeficiency virus infection. *Blood* **2000**, *96*, 3094−3101.
(28) Stamogiannos, A.; Papakyriakou, A.; Mauvais, F. X.; van Endert, P.; Stratikos, E. Screening identifies thimerosal as a selective inhibitor of endoplasmic reticulum aminopeptidase 1. *ACS Med. Chem. Lett.* **2016**, *7*, 681−685.
(29) Saric, T.; Chang, S. C.; Hattori, A.; York, I. A.; Markant, S.; Rock, K. L.; Tsujimoto, M.; Goldberg, A. L. An ifn-gamma-induced aminopeptidase in the er, erap1, trims precursors to mhc class i-presented peptides. *Nat. Immunol.* **2002**, *3*, 1169−1176.
(30) Chang, S. C.; Momburg, F.; Bhutani, N.; Goldberg, A. L. The er aminopeptidase, erap1, trims precursors to lengths of mhc class i peptides by a "molecular ruler" mechanism. *Proc. Natl. Acad. Sci. U. S. A.* **2005**, *102*, 17107−17112.
(31) York, I. A.; Chang, S. C.; Saric, T.; Keys, J. A.; Favreau, J. M.; Goldberg, A. L.; Rock, K. L. The er aminopeptidase erap1 enhances or limits antigen presentation by trimming epitopes to 8-9 residues. *Nat. Immunol.* **2002**, *3*, 1177−1184.
(32) Mansouri, M.; Berger, P. Baculovirus for gene delivery to mammalian cells: Past, present and future. *Plasmid* **2018**, *98*, 1−7.
(33) Koumantou, D.; Barnea, E.; Martin-Esteban, A.; Maben, Z.; Papakyriakou, A.; Mpakali, A.; Kokkala, P.; Pratsinis, H.; Georgiadis, D.; Stern, L. J.; Admon, A.; Stratikos, E. Editing the immunopeptidome of melanoma cells using a potent inhibitor of endoplasmic reticulum aminopeptidase 1 (erap1). *Cancer Immunol. Immunother.* **2019**, *68*, 1245−1261.
(34) Giastas, P.; Neu, M.; Rowland, P.; Stratikos, E. High-resolution crystal structure of endoplasmic reticulum aminopeptidase 1 with bound phosphinic transition-state analogue inhibitor. *ACS Med. Chem. Lett.* **2019**, *10*, 708−713.
(35) Kochan, G.; Krojer, T.; Harvey, D.; Fischer, R.; Chen, L.; Vollmar, M.; von Delft, F.; Kavanagh, K. L.; Brown, M. A.; Bowness, P.; Wordsworth, P.; Kessler, B. M.; Oppermann, U. Crystal structures of the endoplasmic reticulum aminopeptidase-1 (erap1) reveal the molecular basis for n-terminal peptide trimming. *Proc. Natl. Acad. Sci. U. S. A.* **2011**, *108*, 7745−7750.
(36) Stratikos, E.; Stern, L. J. Antigenic peptide trimming by er aminopeptidases–insights from structural studies. *Mol. Immunol.* **2013**, *55*, 212−219.
(37) Sui, L.; Gandhi, A.; Guo, H. C. Crystal structure of a polypeptide's c-terminus in complex with the regulatory domain of er aminopeptidase 1. *Mol. Immunol.* **2016**, *80*, 41−49.
(38) Giastas, P.; Mpakali, A.; Papakyriakou, A.; Lelis, A.; Kokkala, P.; Neu, M.; Rowland, P.; Liddle, J.; Georgiadis, D.; Stratikos, E. Mechanism for antigenic peptide selection by endoplasmic reticulum aminopeptidase 1. *Proc. Natl. Acad. Sci. U. S. A.* **2019**, *116*, 26709−26716.
(39) Mpakali, A.; Giastas, P.; Mathioudakis, N.; Mavridis, I. M.; Saridakis, E.; Stratikos, E. Structural basis for antigenic peptide recognition and processing by endoplasmic reticulum (er) aminopeptidase 2. *J. Biol. Chem.* **2015**, *290*, 26021−26032.
(40) Mpakali, A.; Saridakis, E.; Harlos, K.; Zhao, Y.; Papakyriakou, A.; Kokkala, P.; Georgiadis, D.; Stratikos, E. Crystal structure of insulin-regulated aminopeptidase with bound substrate analogue provides insight on antigenic epitope precursor recognition and processing. *J. Immunol.* **2015**, *195*, 2842−2851.
(41) Mpakali, A.; Maben, Z.; Stern, L. J.; Stratikos, E. Molecular pathways for antigenic peptide generation by er aminopeptidase 1. *Mol. Immunol.* **2019**, *113*, 50−57.
(42) Papakyriakou, A.; Reeves, E.; Beton, M.; Mikolajek, H.; Douglas, L.; Cooper, G.; Elliott, T.; Werner, J. M.; James, E. The partial dissociation of mhc class i-bound peptides exposes their n terminus to trimming by endoplasmic reticulum aminopeptidase 1. *J. Biol. Chem.* **2018**, *293*, 7538−7548.
(43) Chen, H.; Li, L.; Weimershaus, M.; Evnouchidou, I.; van Endert, P.; Bouvier, M. ERAP1-ERAP2 dimers trim MHC I-bound precursor peptides; implications for understanding peptide editing. *Sci. Rep.* **2016**, *6*, 28902.
(44) Maben, Z.; Arya, R.; Rane, D.; An, W. F.; Metkar, S.; Hickey, M.; Bender, S.; Ali, A.; Nguyen, T. T.; Evnouchidou, I.; Schilling, R.; Stratikos, E.; Golden, J.; Stern, L. J. Discovery of selective inhibitors of endoplasmic reticulum aminopeptidase 1. *J. Med. Chem.* **2020**, *63*, 103−121.
(45) Halberg, M. Targeting the insulin-regulated aminopeptidase/AT4 receptor for cognitive disorders. *Drug News Perspect.* **2009**, *22*, 133−139.
(46) Waterman, D. G.; Winter, G.; Gildea, R. J.; Parkhurst, J. M.; Brewster, A. S.; Sauter, N. K.; Evans, G. Diffraction-geometry refinement in the dials framework. *Acta Crystallogr. D Struct Biol.* **2016**, *72*, 558−575.
(47) Evans, P. R.; Murshudov, G. N. How good are my data and what is the resolution? *Acta Crystallogr., Sect. D: Biol. Crystallogr.* **2013**, *69*, 1204−1214.
(48) Winn, M. D.; Ballard, C. C.; Cowtan, K. D.; Dodson, E. J.; Emsley, P.; Evans, P. R.; Keegan, R. M.; Krissinel, E. B.; Leslie, A. G.; McCoy, A.; McNicholas, S. J.; Murshudov, G. N.; Pannu, N. S.; Potterton, E. A.; Powell, H. R.; Read, R. J.; Vagin, A.; Wilson, K. S. Overview of the ccp4 suite and current developments. *Acta Crystallogr., Sect. D: Biol. Crystallogr.* **2011**, *67*, 235−242.
(49) Smart, O. S.; Womack, T. O.; Flensburg, C.; Keller, P.; Paciorek, W.; Sharff, A.; Vonrhein, C.; Bricogne, G. Exploiting structure similarity in refinement: Automated ncs and target-structure restraints in buster. *Acta Crystallogr., Sect. D: Biol. Crystallogr.* **2012**, *68*, 368−380.
(50) Emsley, P.; Lohkamp, B.; Scott, W. G.; Cowtan, K. Features and development of coot. *Acta Crystallogr., Sect. D: Biol. Crystallogr.* **2010**, *66*, 486−501.

https://dx.doi.org/10.1021/acs.jmedchem.9b02123
J. Med. Chem. XXXX, XXX, XXX−XXX